Bioimpedance MR Scanning For Hypertension and Functional Experience

R.Kalaivani
Principal, MIT College of Arts and Science for Women
Musiri, Trichy, Tamil Nadu, India
kalairamesh81@gmail.com

J.Premalatha
Department of Electronics and Communications Engineering, Chennai Institute of Technology
Chennai, Tamil Nadu, India
prema.joe@gmail.com

B.Gopi
Department of Electronics and Communication Engineering, Muthayammal Engineering College (Autonomous)
Rasipuram, Tamil Nadu, India.
bgbalasampath@gmail.com

V.Prasanna Srinivasan
Department of Information Technology, R.M.D Engineering College
Kavaraipettai, Chennai, Tamil Nadu, India
vas.sri81@gmail.com

Ravikumar D
Department of Electronics and Communications Engineering, Kings Engineering College,
Irugattukotai, Chennai, Tamil Nadu, India
ravikumar.dinakaran@gmail.com

S. Renukadevi
Department of Mathematics, Bharathi Women's College (Autonomous),
Chennai, Tamil Nadu, India
dr.s.renukadevi@gmail.com

2022 International Conference on Computer, Power and Communications (ICCPC) | 979-8-3503-9784-0/22/$31.00 ©2022 IEEE | DOI: 10.1109/ICCPC55978.2022.10072065

Abstract—**Present anatomy detection solutions generally use data mining techniques to use large annotated datasets to learn how anatomy is detected. These solutions are subject to various constraints, including the use of suboptimal techniques in function development and the influence of technologically inappropriate anatomy detection search schemes. To deal with those problems, a process pursuing a new model in which the identification problem is reformulated as an artificial agent learning task is suggested. The anatomy model and object study with deep strengthening learning with the capabilities of multi-scale image processing in a single behavioral context are integrated. This approach tested over 1 million image slices, demonstrating that, although it increased detection precision by 20-30 percent, it dramatically outperformed state-of-the-art solutions to identify different anatomical constructions without loss from a clinical acceptance perspective. By 2-100 magnitude orders for the detection speed in comparison methods, guaranteeing that large three-dimensional scans produce unparalleled real-time performance is strengthened.**

Keywords— Filter Bank, Boltzmann classification methods, Texture Recognition Algorithm, Lung CT images.

I. INTRODUCTION

Solid and quick identification of radiographic images is a pre-condition for diagnostic and medical review of the interventional image. For computer-aided diagnostic, detection of anatomic monuments is a prerequisite [1]. The image-to-image registration structure tracks the developed country modelers and mechanical simulations to initialize and limit maths for gravimetric organ segmentation. Many clinical support applications need to be accurate and auto-sensitive [2]. This means that the physician can assist with automated observations to detect fast and reliable anatomical signs for more efficient and streamlined image reading. On 3D-CT this is concentrated, an image analysis advanced technology used for both interventional and diagnostic applications [3]. In other words, an autonomous agent has been learned to discern the object's anatomy from the individual and locate the object in the image volumetric space by studying and following the ideal route of navigation to the target object [4].

Typically, the current anatomical landmark detection solutions are based on mathematical concepts, which effectively use large annotating medical image database systems. Therefore, the indicator is generally disconnected in two separate and synchronous stages: to learn the optimization technique and search the object [5]. The first step is to obtain the image information behind it and use it as Sci. proof to recognize the anatomical mark. To do this, conventional neural networks rely on precise supervised classification strategies to understand image information with human ingenuity [6].

The learning models enable the complicated anatomical variation to be better captured, improved efficiency, and widespread data. However, the methods above depend on comprehensive one-shot-shot scanning assessment or later part image mapping techniques that lead to false detection and unrealistically high calculation times [7].

This introduces a solution based on a new detection process as a compartmental follows a different paradigm. Using deep strengthening theory and the theory of scale, different spatial resolutions via the image's voxel-grid, i.e. image representation by scale and converge to the desired location can be used [8].

This formula uses the different abstract levels encoded systematically and naturally. The search begins on the scale with a globalized world and keeps going across scales, with increasing data when making the transition as additional evidence. The most exclusionary imaging features visibility on each of the scale levels, the use of independent search modelling techniques is proposed [9].

The network functions by selecting a unit and frequently resetting its state. After a specified amount of time has passed at a certain temperature, the chance of the network being in a global state is calculated only by the energy of that global state, as determined by a Boltzmann distribution, rather than the starting state from which the process began. This suggests that the energy of global state log-probabilities will become linear as a result. This link is maintained when the device is said to be "at thermal equilibrium." This means that the probability distribution of all global states has converged. After beginning at a high temperature, the temperature of the network gradually declines until it reaches a lower temperature where it achieves a state of thermal equilibrium. It's possible that the distribution will eventually settle on one in which the energy level fluctuates about the global minimum. In principle, the Boltzmann machine may act as a stand-in for any kind of computing media. For instance, if the machine is taught on photos, it may theoretically model the distribution of photographs and use

that model to complete an incomplete photograph if it has been trained on those images.

II. Literature Survey

The key category of sensing solutions, especially in 3D data, is the scanning-based devices. A classificatory is the position where the negative hypotheses H− are educated and the presence of the object being searched is basically differentiated from the rest of the sampled anatomy [10]. Classic models of machine learning, highly random trees and probabilistic development of trees or deep learning, deep neural networks and sparse adaptive deep neural networks can be used [11]. Aggregating hypotheses can obtain the final outcome with Hough regression or by combining.

But for exercises with a great range of high resolution 3D-CT body scans, the theories used to practise can outweigh the existing GPU systems' memory capabilities. In addition, the classifier is used during test time to search the entire size of a certain image as a series exponentially increasing with image dimensions [12]. The selection uncertainty approaches billions in the case of a volume with a hypothesis of 15 15 15. This approach can also be responsive to false positives in classifiers and is often combined with different methods such as filtering by cascade and filtering simultaneously, or active planning to facilitate effective 3D data formation and detection. This approach is often combined with different methods [13].

The End-to-End Systems, known as image-to-image technologies, are based on the architectures of the whole network (FCN), which allow us to map the original image to the segmentation of multi-masks or image codes that emphasise the anatomy [14]. A region-based FCN method for effective object detection was recently proposed by Dai et al. While these solutions allow the simultaneous pixel/voxel classification and enable multiple landmark identification, the training is highly versatile about the both memory administration and processing time [15]. For example, a CT scan containing 3 20 20 125 voxels in a standard FCN might transfer a computational cost of 3-4 GB for a forward-looking procedure – which seriously reduces the sampled lot of images throughout training. In this quickly progressing field of science, these issues are resolved, including retention difficulties.

Regression Systems take advantage of the site's anatomical background to learn relative vectors of displacement pointing to the site. Random forest regression, deep coevolutionary neural networks, or current spatial transformation neural networks may be used to learn visualization. Although these solutions significantly increase the performance of scan-based devices, the variants of the scanning spectrum are inherently difficult to train and not stable.

To overcome the localization tasks, Atlas-based device registry and multi-atlas registration methods can also be used. However, the application for large 3D-CT scans raises major computing problems with limited model optimization. Potential et al. overcome this constraint using dense part-based compliant graphic templates by choosing the functionality between the area suggestion and the tracking network by reducing the estimation time. Usage of FCNs has contributed to further runtime changes. Deep learning solutions for human location prediction have already produced state-of-the-art results. Two frequent targets are the CPMs for sequential forecasting and the coevolutionary Layered Hourglass networks.

Visually and tactilely, the texture may be differentiated from one another. Tactile texture refers to the how a surface really feels, as opposed to visual texture, which refers to how the form or contents of an image seem to the viewer. Texture identification is a relatively straightforward operation inside a human vision system; however, the machine vision domain and image processing are more difficult. When it comes to image processing, the texture may be analysed and defined as a function of the spatial variation of the brightness intensity of the pixels. Each level's changes are represented by the texture, which assesses properties like smoothness, smoothness, coarseness, and regularity of each surface in distinct order directions.

III. Proposed System

Designers suggest that anatomical object detection be redefined as a behavioral problem show brilliant characterizes this system's capacity to discover and think about locating an entity, rather than pursuing predefined detailed search strategies. To do this, semantic simulation principles based on better learning are paired with spatial processing and machine learning.

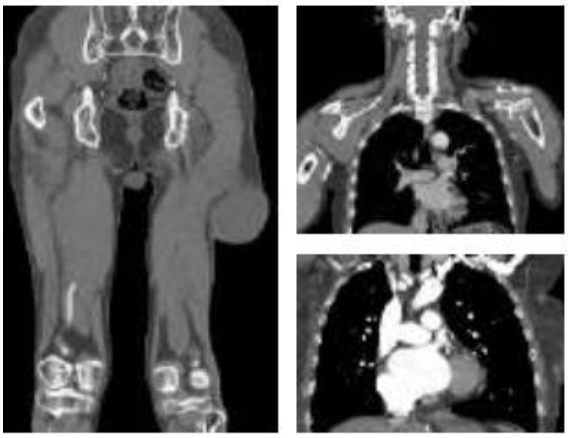

Fig. 1. Sample Medical Scan Images.

Figure 1 shows the sample medical scan images. Imaginary influence of contemporary Classification algorithms and cognitive stimulation through enhancement learning will be incorporated. Initially, under the name deep enhancement learning, a process used to train artificial agents for mastering various ATARI games, the synthesis of these two components was described in literature. It is recommended that anatomy identification be reformulated as an artificial agent cognitive learning activity. It can be looked for voxel-based navigation paths from any arbitrary p-to-p-filing point with an action-value function Learning property Q-fil enabling an agent efficiently to locate items in the image rather than to thoroughly digitize the volumetric field. An appropriate environmental exploration is used as a learning process to ensure a random exploration by an off-political approach. This implies that the acts are chosen either in a random probability 1 s uniformly during preparation. In the tests, the present early annuals from 1.0 to 0.05 to correlate with probability s or deterministically are

used. Figure 2 shows the proposed bio-impedance MR scanning for hypertension and functional experience.

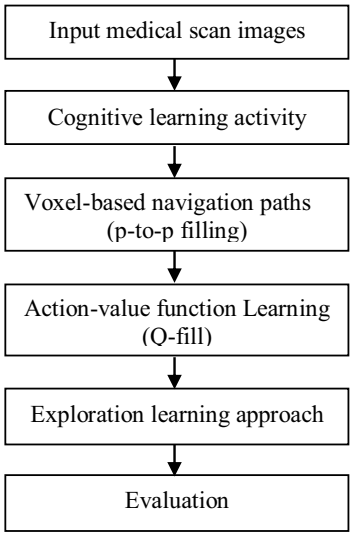

Fig. 2. Proposed System Performance Analysis.

Another main technique is decorrelation of class labels using the principle of managed learning to guarantee the stability oscillations Mi = [T1, T2] during preparation that is still there. Extended and sampled consistently to measure the degree of learning. To use adjustable episode duration to speed up the preparation further is proposed. By decreasing episode length steadily during training utilizing linear decay this is noticed, it is enhanced discovery by sampling more and more trajectories retained in the active memory.

By analytical study, it is observed that this basic adjustment improved the strength of the educated policy and cut the practice time by about 30 percent on average. This is because the policy changes during workouts and the sampled paths merge quicker through the field, removing any need for external appearance episodes that may influence the probabilistic sample to approximate gradients. 1000 first steps and eventually 50 steps in the first duration of the episode are had. Given this device concept, a major constraint in the simulation of State Space S may be found in particular in the form of an image strength box in the acquired state image's size.

Obtaining a small, locally only accessible box would increase the reliability of the sampling. It is very important to learn an appropriate policy on navigation. On the opposite, removing a very huge container to make the laws presents big computer problems in 3D space. This concession reveals the failure to accurately use the image details on multiple scales from the conceptual methodology.

IV. Results and Discussions

A collection comprises a total of 2224 three-dimensional quantities from 280 patients, including a wide array of scan forms, e.g., heart CT scans (contraction), chest scans, abdominal scans, leg CT scans, and head and neck CT scans. A substantial portion of these scans was centered in the chest and abdomen regions, spanning the whole person by about 20 percent. In fact, whole anatomy images are also only obtained in unusual circumstances to facilitate rapid accident examinations in patients with polytrauma.

Different fractures and tumours in the leg, thorax CT scans, abdominal and pelvis scans for cancer, and so on. As such, amounts have been re-sampled to isotropic frequency of 2 mm major tumours or abnormalities in several of the scans. Both are at the finest standard in the legal representative before the stage. 0.5 mm, 1 cm and 2 mm space resolutions. Table 1 clearly shows the performance of system in terms of classification accuracy for different training samples.

TABLE I. Performance of the Proposed System with 50 Steps

Space resolution	Accuracy (%)				
	Training samples (%)				
	Ten	Twenty	Thirty	Forty five	Sixty
0.5	93.17	89.00	85.05	79.08	73.44
1	95.33	91.83	88.25	82.11	76.33
1.5	96.92	93.70	90.25	85.03	80.93
2	98.53	95.91	92.75	88.22	81.99
2.5	99.19	98.20	96.50	92.92	89.46

TABLE II. Performance of the Proposed System with 100-Neighbour

Space resolution	Accuracy (%)				
	Ten	Twenty	Thirty	Forty five	Sixty
0.5	95.36	92.54	89.05	84.05	78.55
1	96.56	93.76	90.18	84.67	79.32
1.5	97.33	94.72	91.02	85.97	81.27
2	98.44	95.61	92.72	87.54	82.10
2.5	99.47	98.39	96.88	93.51	90.00

It can be seen that the performance of system using 100 steps in the first duration classifies the images with an accuracy of 99.47% whereas 50-steps provides 99.19%. It is also noted that for all combinations, 100-steps provides promising results than 50-steps. Figure 3 clearly shows the results of 100-steps graphically.

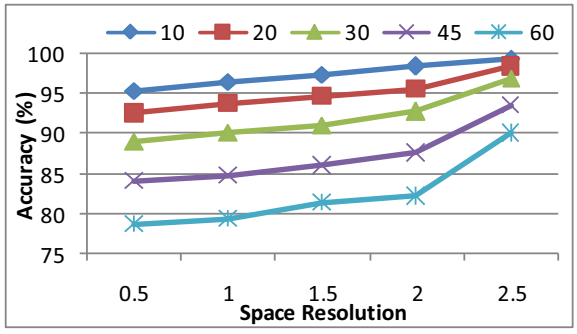

Fig. 3. Results of the systems graphically at 5-steps at first.

This interval into unit range for these scale-space are clipped into, i.e. [0, 1], by 3 additional levels. A set of 8 anatomical points of reference, and vessel dichotomy and bifurcation of the respiratory tract, has been chosen for the useful 0-15000 HU interval. voxel values. The middle of the left and right renal, bronchial fork, the front of the hip bones

left and right, and the three artery bifurcations between the left subclavian arteries and aortic, brachiocephalic arteries, and the left carotid are involved.

In addition to its ability to accommodate significant differences in non-starring organs, the anatomical configuration and the uncertainty of nearby vessel bifurcations of analogous appearance was checked. Radiologists provided surface descriptions. The fork and bone markings of vessels are physiologically clearly defined, such that very detailed notes with an actual level can be made. The recorded average inter-server variability was at 1 mm with respect to bone landmarks, while the intra-server variability was 0.9 mm with three specialist annotators.

This degree of consistency is consistent with the outcomes of the analysis. On the other hand, the shift in the annotation of the kidney core is larger than the structure's scale. The inter-user variation is usually low for certain landmarks as well. The division was made at the patient stage, indicating all scans in the classification model or in the test set of a single patient.

V. Conclusion

A novel way of precise anatomical detection in 3D CT scans in real-time is unveiled. The theory of profound machine learning with microcomputer vision is inconsistently learned but can be combined using a generic behavioral learning task. Experiments display that the results are robust with outliers and achieve an average of 20-30 percent better precision than the ones used. Simultaneously, this algorithm's detection speed is 2-3 magnitude orders faster and reaches real-time performance for 3D-CT volumes. The alternative can also manage missing objects eloquently and can be lengthened to allow multiple objects to be detected simultaneously. The new framework could comprise an enormous portion of the clinical technologies of the next decade to contribute to better, cheaper, and more reproductive patient treatment plans, therapy, and infection control, through high strength and full detail. The evaluation configuration is based on the probability division of the volumes annotated in around 80% of the training sessions, with 20% of test examples unknown for each guide. The applicability of 3D CT can be discovered in congenital or traumatic bone diseases. It is particularly helpful in defining specific bone outlines and allows the doctor to organize his approach with the assistance of lifelike renderings of bony components. With the effective use of this technology in such instances at our center and the good reaction from doctors, it has become a common application in the imaging work-up for the indications discussed previously. Before referring a patient for 3D CT examinations, the doctor must have a thorough understanding of the indications as well as the potential traps in the nature of artifacts.

References

[1] T. Svtern, M. Ebner, and Urschler, "From local to global random regression forests: Exploring anatomical landmark localization," Medical Image Computing and Computer-Assisted Intervention, vol. 9901, pp. 221–229, 2016.

[2] R. Gauriau, D. Cuingnet, I. Lesage, and Bloch, "Multi-organ localization with cascaded global-to-local regression and shape prior," Medical Image Analysis, vol. 23, no. 1, pp. 70–83, 2015.

[3] A. Bengio, P. Courville, and Vincent, "Representation learning: A review and new perspectives," IEEE Transactions on Pattern Analysis and Machine Intelligence, vol. 35, no. 8, pp. 1798–1828, 2013.

[4] D. Payer, H. Svtern, M. Bischof, and Urschler, "Regressing heatmaps for multiple landmark localization using CNNs," Medical Image Computing and Computer-Assisted Intervention, vol. 9901, pp. 230–238, 2016.

[5] S. S. Abdulkadir, T. Lienkamp, O. Brox, and Ron-Neberger, "3D U-net: Learning dense volumetric segmentation from sparse annotation," Medical Image Computing and Computer-Assisted Intervention, vol. 9901, pp. 424–432, 2016.

[6] D. Zheng, B. Liu, H. Georgescu, D. Nguyen, and Comaniciu, "3D Deep learning for efficient and robust landmark detection in volumetric data," Medical Image Computing and Computer- Assisted Intervention, vol. 9349, pp. 565–572, 2015.

[7] K. Mnih, D. Kavukcuoglu, A. A. Silver, J. Rusu, M. G. Veness, A. Bellemare, M. Graves, A. K. Riedmiller, G. Fidjeland, S. Ostro-Vski, C. Petersen, A. Beattie, I. Sadik, H. Antonoglou, D. King, D. Kumaran, S. Wierstra, D. Legg, and Hassabis, "Human-level control through deep reinforcement learning," Nature, vol. 518, no. 7540, pp. 529–533, 2015.

[8] Lindeberg, pp. Scale-Space Theory in Computer Vision. Springer US, 1994, ch. Scale-space for N-D discrete signals, pp. 101–122, 1994.

[9] B. Gesu, T. Georgescu, D. Mansi, J. Neumann, D. Hornegger, and Comaniciu, "An artificial agent for anatomical landmark detection in medical images," Medical Image Computing and Computer-Assisted Intervention, vol. 9902, pp. 229–237, 2016.

[10] F. Joseph and M. Subbiah, "Hybrid windowing adaptive FIR filter technique in underwater communication," International Journal of MC Square Scientific Research, vol. 10, no. 2, pp. 17–21, 2018.

[11] Q. Dai, G. R. Yang, Y. Xue, and Yu, "Boosting for transfer learning," Proceedings of the 24th international conference on Machine learning, pp. 193–200, 2007.

[12] Z. Kenig, A. Kam, and Feuer, "Blind image deconvolution using machine learning for three-dimensional microscopy," IEEE Trans. Pat- tern Anal. Mach. Intell, vol. 32, no. 12, pp. 2191–2204, 2010.

[13] X. Wong, X. Su, C. M. G. Li, R. Cheung, C.-Y Klein, T. Y. Cheng, and Wong, "Global prevalence of age-related macular degeneration and disease burden projection for 2020 and 2040: a systematic review and meta-analysis," The Lancet Global Health, vol. 2, no. 2, pp. 106–116, 2014.

[14] H. A. D. Boer, M. A. Vrooman, M. W. Ikram, M. Vernooij, A. Breteler,V. Der, W. J. Lugt, and Niessen, "Accuracy and reproducibility study of automatic MRI brain tissue segmentation methods," Neuroimage, vol. 51, no. 3, pp. 1047–1056, 2010.

[15] S. Murugan, T. R. G. Babu, and C. Srinivasan, "Underwater Object Recognition Using KNN Classifier," International Journal of MC Square Scientific Research, vol. 9, no. 3, pp. 48–52, 2017.